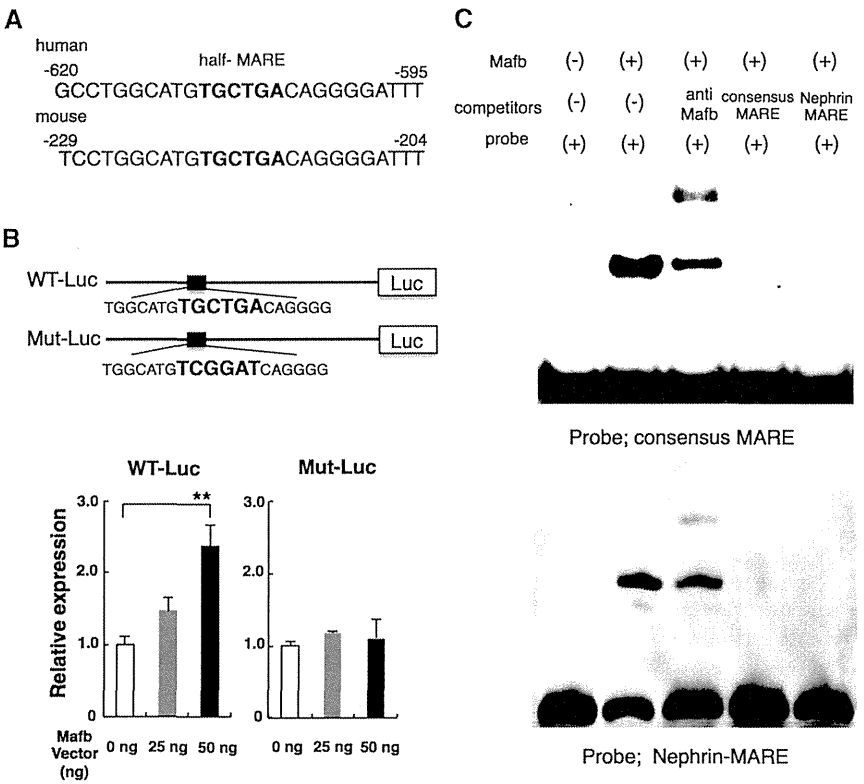

Figure 4. Mafb directly regulates Nephrin expression. (A) Analysis of the 5′-flanking region of Nephrin by the Ensembl Genome Database Web site identified an Mafb binding site (half-MARE) that is highly conserved between mouse and human (Nephrin-MARE). (B) Reporter assay. WT Nephrin-MARE (WT-Luc) and mutated Nephrin-MARE (Mut-Luc) luciferase reporter constructs are indicated. The 293T cells were cotransfected with the indicated Nephrin promoter–reporter plasmid constructs along with the Mafb expression plasmid, and the relative luciferase activity was measured as described in Concise Methods. The relative luciferase activity of the reporter plasmids is shown in the lower panel with the activity generated from cells transfected with the empty reporter vector (0 ng) and the Mafb expression plasmid defined as 1.0. Each bar represents the mean±SEM. $^{**}P<0.05$. (C) EMSA using labeled consensus MARE (upper panel) and Nephrin-MARE (lower panel). (Lane 1) Biotin-labeled consensus MARE probe. (Lane 2) Mafb protein and biotin-labeled consensus MARE probe. (Lane 3) Lane 2+anti-Mafb antibody. (Lane 4) Lane 2+unlabeled consensus MARE oligonucleotide. (Lane 5) Lane 2+unlabeled Nephrin-MARE oligonucleotide.

reported that MAFB mutations cause MCTO. Patients with MCTO often progress to end stage kidney disease.[11] Because some of the cases showed FSGS,[27] renal failure might be attributed to podocyte dysfunction caused by MAFB mutations.[11] The *Mafb* gene has been reported to localize to the vicinity of the albuminuria-susceptible locus in diabetic mice.[12] These facts suggest Mafb might play an important role in diabetic nephropathy. In this study, we analyzed diabetic Mafb TG mice. We found that Mafb overexpression might ameliorate diabetic nephropathy through Nephrin, Gpx3, and Notch2 in podocytes.

Nephrin, the key molecule of the glomerular slit diaphragm, is expressed on the surface of podocytes and critical in preventing proteinuria.[1] In diabetes, hyperglycemia leads to the loss of surface expression of Nephrin and causes proteinuria in human diabetic nephropathy and rodent STZ-induced diabetic model.[28,29] Although the mechanism of Nephrin loss remains unclear, hyperglycemia induces protein kinase C α-mediated Nephrin endocytosis.[30] In this study, we found that Mafb overexpression significantly attenuated Nephrin loss in diabetic mice. Moreover, it was observed that Mafb stimulates Nephrin transcription through an MARE within the proximal promoter of the Nephrin gene. Several studies have shown that Nephrin is regulated at the transcriptional level.[14,16,17] Guo *et al.*[16] reported that a 186-bp fragment of the human Nephrin promoter containing retinoid X receptor/retinoic acid receptor and WT1 response elements is capable of directing podocyte-specific expression. An MARE is also located within this fragment. Our data suggest that Mafb signaling is an important regulator of the Nephrin promoter. However, we could not identify MAREs within the 5′-flanking regions of *Gpx3* or *Notch2*. The mechanism by which Mafb regulates *Gpx3* and *Notch2* expressions thus remains to be determined. Additional studies and other supporting data are needed to clarify the precise biologic properties of Mafb.

Gpx, which is an antioxidative stress enzyme, was elevated in Mafb TG glomeruli. It has been suggested that oxidative stress constitutes a key and common event in the pathogenesis of diabetic nephropathy.[31] Antioxidant administration has been shown to have potential beneficial effects in human and experimental diabetic nephropathy.[32–35] A recent study suggested that Gpx3 is produced by podocytes and interacts with podocin.[21] The mRNA expression of *Gpx3* was significantly reduced in glomeruli after puromycin aminonucleoside nephropathy induction.[20] Our data suggest Mafb overexpression in podocytes might ameliorate diabetic nephropathy through Gpx3.

We also found that Notch2 expression was increased in diabetic Mafb TG glomeruli. In contrast, the expression of Notch1, Notch ligands, and Notch target genes was decreased. *NOTCH2* has been identified as a primary *MAFB* target gene.[24] Several recent studies described the expression of Notch pathway proteins in kidneys of patients with diabetic nephropathy.[25,36] Expression of Notch1 in podocytes causes the development of albuminuria and glomerulosclerosis,

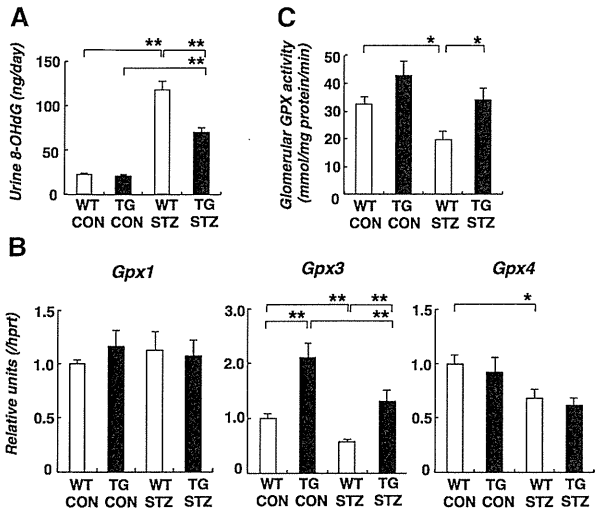

Figure 5. Oxidative stress was improved through Gpx activity in diabetic Mafb TG mice. (A) The urinary 8-OHdG level in TG STZ mice was significantly decreased compared with WT STZ mice. (B) Gpx expression in diabetic glomeruli by quantitative RT-PCR analysis. *Gpx3* expression was increased in TG CON glomeruli. The diabetes-induced reduction in *Gpx3* expression was mitigated in TG STZ glomeruli. (C) Glutathione peroxidase activity in the glomeruli. The reduction in Gpx activity in WT STZ was mitigated in TG STZ glomeruli. Values represent the means±SEMs (n=4 mice per group). *P<0.05; **P<0.01.

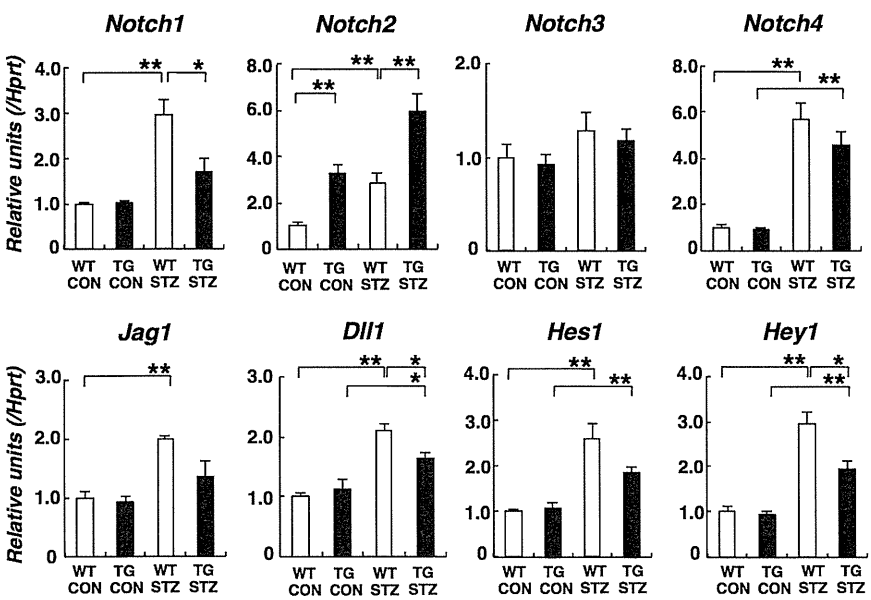

Figure 6. Notch2 expression was increased in diabetic glomeruli, and this effect was enhanced in diabetic Mafb TG glomeruli. Analysis of Notch signaling expression by quantitative RT-PCR in diabetic Mafb TG glomeruli. We observed increased expression of *Notch1* and *Notch4*, Notch ligands (*Jag1* and *Dll1*), and Notch target genes (*Hes1* and *Hey1*) in WT STZ glomeruli. The fold induction of these genes was mitigated in TG STZ glomeruli. Meanwhile, glomerular *Notch2* expression was increased in TG CON mice. *Notch2* expression was further potentiated in TG STZ mice. Values represent the means±SEMs (n=4 mice per group). *P<0.05; **P<0.01.

whereas genetic deletion or pharmacological inhibition ameliorates diabetic nephropathy in murine models.[25] *In vitro* and *in vivo* studies showed that Notch1 induces apoptosis of podocytes through the activation of p53.[25,37] Meanwhile, Notch2 elevation in podocytes has also been observed in human and experimental diabetic nephropathy.[25,38] However, the *in vivo* role of Notch2 in podocytes is poorly understood. Increased renal tubulointerstitial Notch1 levels are associated with increased fibrosis and decreased renal function, whereas tubulointerstitial expression of Notch2 is associated with samples with less fibrosis and better renal function in CKD.[38] These results would suggest that, similar to tubulointerstitial fibrosis, Notch1 and Notch2 in podocytes might have different roles in diabetic nephropathy as well. An opposing role between Notch1 and Notch2 has been observed in other diseases. For example, in colorectal cancer, high expression of Notch1 is associated with poor overall survival, whereas high expression of Notch2 predicts better survival.[39] Additional studies are needed to elucidate the role of Notch2 in podocytes and the interaction between Notch1 and Notch2. A recent study showed Mafb–green fluorescent protein bacterial artificial chromosomes in TG mice. The work by Brunskill *et al.*[40] represents microarrays of podocytes from embryos at embryonic day (E) 13.5 and E15.5 as well as adults. The report will be useful to analyze additional targets for Mafb.

Loss of podocytes contributes to the progression of diabetic nephropathy. Podocyte apoptosis is known as one cause of podocyte depletion.[1] We observed that apoptotic podocytes were decreased in diabetic Mafb TG glomeruli. Notch signaling changes and antioxidant protection by Mafb might induce the antiapoptotic effects. Mafb expression has been shown to confer antiapoptotic effects in myeloma and macrophage cell lines.[24,41]

In summary, we showed in the present study that Mafb might play a protective role in diabetic nephropathy. This effect is regulated through slit-diaphragm proteins, antioxidative enzymes, and Notch pathways in podocytes. We, therefore, suggest that an increased Mafb activity is of pivotal importance for the development of diabetes nephropathy. Mafb could be a therapeutic target in diabetic nephropathy.

CONCISE METHODS

Mice

We generated TG mice that overexpress Mafb in podocytes using the human Nephrin promoter/enhancer.[13] Eight-week-old WT and Mafb TG mice were treated with either STZ or saline solution. After 12 weeks of treatment, diabetic

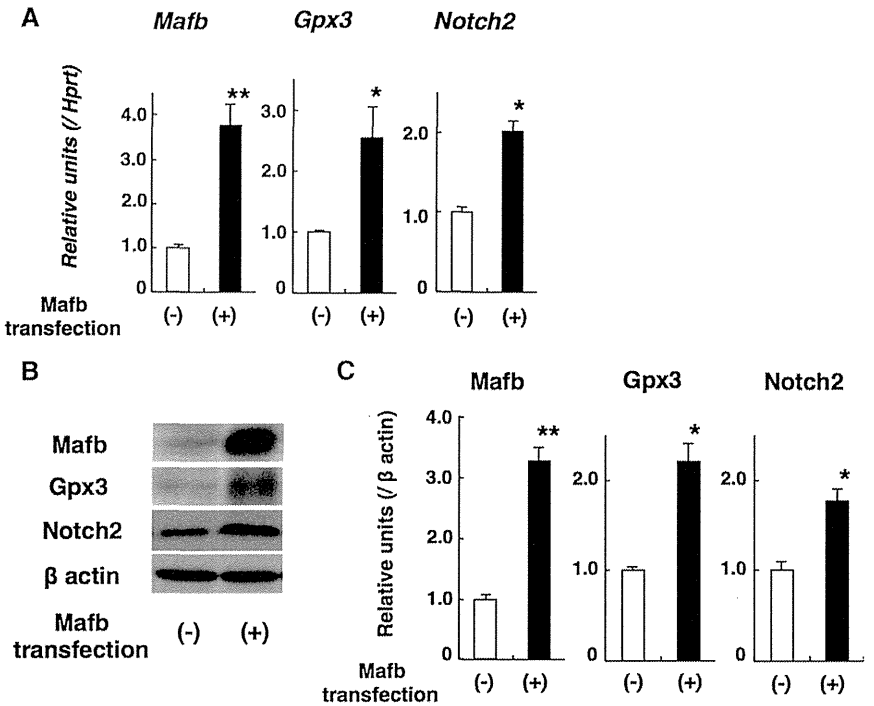

Figure 7. Mafb upregulates Gpx3 and Notch2 expression in cultured podocytes. (A) Quantitative RT-PCR analysis. *Gpx3* and *Notch2* elevation was observed in Mafb-transfected podocytes. (B) Representative Western blotting of Mafb, Gpx3, and Notch2. (C) Graph depicting quantitative analysis by Western blot. Gpx3 and Notch2 elevation was found in Mafb-transfected podocytes. Values represent the means±SEMs (n=3 per group in independent experiments). *P<0.05; **P<0.01.

nephropathy was assessed by biochemical analyses of urine, serum, and histologic analyses of the kidneys. Diabetes was induced by a single intraperitoneal injection of STZ (150 mg/kg body wt; Sigma-Aldrich, St. Louis, MO) that had been diluted in citrate buffer (pH 4.5). Control mice were injected with an equal volume of citrate buffer alone. After 7 days, the induction of diabetes was confirmed by the measurement of blood glucose concentrations. Fed animals with blood glucose levels that were greater than 300 mg/dl were considered to be diabetic. Mice were maintained in the Laboratory Animal Resource Center. All experiments were performed according to the Guide for the Care and Use of Laboratory Animals of the University of Tsukuba.

Southern Hybridization Analysis of Genomic DNA

High-molecular weight DNA was prepared from the tail of each mouse, and 25 μg DNA was digested with *EcoR*I and then electrophoresed through 1.0% agarose gels. After electrophoresis, the DNA was transferred to a nylon membrane (Hybond-N^+; GE Healthcare Life Sciences, Little Chalfont, UK). Southern hybridization was performed using digoxigenin-labeled DNA probes that were amplified using forward (5′-TGAGCATGGGGCAAGAGCTG-3′) and reverse (5′-CCATCCAGTACAGGTCCTCG-3′) oligonucleotide primers in hybridization buffer at 42°C overnight. After hybridization, probes were detected using alkaline phosphatase-conjugated antidigoxigenin antibody (Roche Diagnostics, Basel, Switzerland). Transgene copy number was determined from the blot with ImageJ (National Institutes of Health, Bethesda, MD).

Western Blot Analysis of Kidneys

Nuclear extracts were prepared from the kidneys of 10-week-old WT or TG mice. The extracts were fractionated by size on a 10% SDS–polyacrylamide gel, transferred to a polyvinylidene difluoride membrane (EMD Millipore Corporation, Billerica, MA), and incubated with primary and secondary antibodies. To detect the Mafb protein, a rabbit antibody against mouse Mafb (BL658; Bethyl, Montgomery, TX) was used as the primary antibody, and peroxidase-conjugated goat anti-rabbit IgG (Invitrogen, Carlsbad, CA) was used as the secondary antibody. To normalize the results with respect to the amount of protein in each sample, a goat antibody against mouse Lamin B (C-20; Santa Cruz Biotechnology, Dallas, TX) was used. Amount of proteins was determined from the blot with ImageJ.

Measurements of Serum Glucose and Insulin

The serum concentration of glucose was measured using a Dry-Chem 3500 automated analyzer for routine laboratory tests (FujiFilm Inc., Tokyo, Japan). The serum insulin levels in fed animals were measured with a rat insulin ELISA kit (Morinaga Institute of Biologic Science, Yokohama, Japan).

Analysis of Urinary Albumin Excretion and Renal Serological Assays

The urine of each mouse was collected in an individual metabolic cage over a 24-hour period. Urinary albumin was measured using the Albuwell M ELISA quantitation kit according to the protocols by the manufacturer (Exocell, Philadelphia, PA). The serum concentration of BUN and creatinine were measured using a Dry-Chem 3500 automated analyzer.

Histopathological Analysis of Renal Tissues

Each mouse was bled while under ether anesthesia. At autopsy, organs were fixed with 10% formalin in 0.01 mol/L phosphate buffer (pH 7.2) and embedded in paraffin. Sections were stained with Periodic acid–Schiff stain and Masson's trichrome staining for histopathological examination under light microscopy. For immunofluorescence analysis, frozen sections were stained with anti-Nephrin, anti-Podocin and anti-Mafb as previously described.[10] Quantitative estimation of immunofluorescence was performed using ImageJ. Relative fluorescence intensity was calculated using the mean fluorescence intensity of nondiabetic WT mice defined as 1.0.

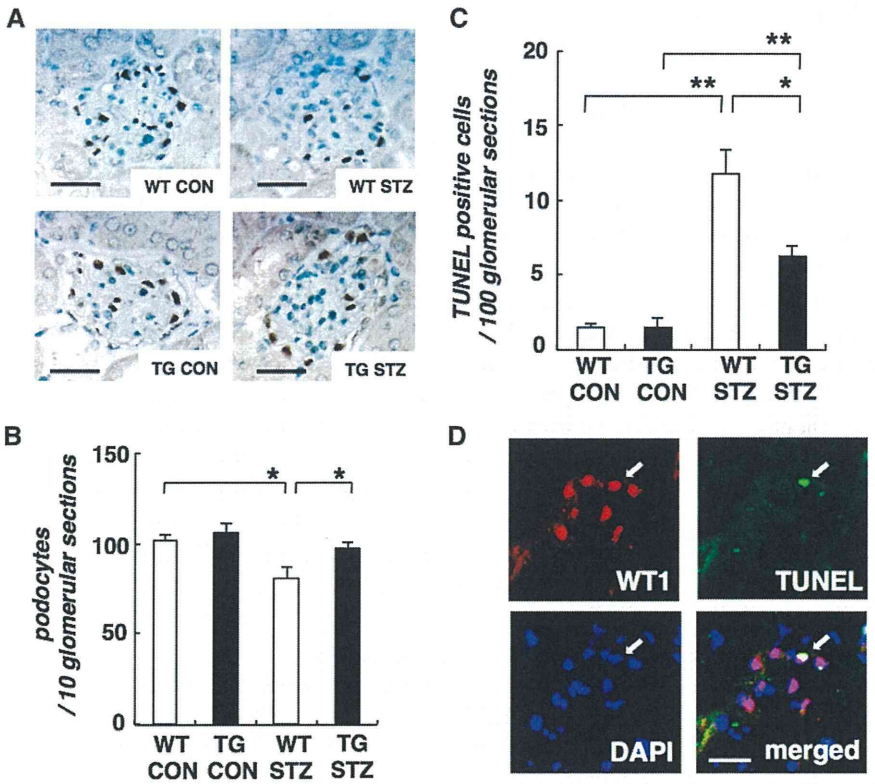

Figure 8. Overexpression of Mafb partially restores podocyte number. (A) Typical images of WT1-stained glomeruli from WT CON, TG CON, WT STZ, and TG STZ mice. (B) Average number of WT1-stained nuclei calculated per glomerular sections. The number of WT1-stained nuclei was obtained from 10 glomerular sections per kidney sample. Values represent the means±SEMs (n=4 mice per group). *P<0.05. (C) Diabetes-induced glomerular cell death is reduced by Mafb overexpression. TUNEL staining in WT CON, TG CON, WT STZ, and TG STZ glomeruli. Quantification of TUNEL staining in all glomerular sections per kidney sample. Values represent the means±SEMs (n=4 mice per group). *P<0.05; **P<0.01. (D) Apoptotic glomerular cells were podocytes in diabetic glomeruli. TUNEL-positive apoptotic podocyte in the glomeruli of WT STZ mice was WT1-positive (arrows). Blue, 4′,6-diamidino-2-phenylindole (DAPI); green, TUNEL; red, WT1. Scale bar, 50 μm.

Glomerular Surface Area Determination

The glomerular surface area of 20 glomeruli in each kidney section was measured using a BIOREVO BZ-9000 microscope (Keyence, Osaka, Japan), and the mean glomerular surface area was calculated.

Tubulointerstitial Morphology

The index of renal tubulointerstitial damage was graded with the experimental protocol using a light microscope on a scale of grades 0–4 (grade 0, normal; grade 1, affected area<10%; grade 2, affected area=10%–25%; grade 3, affected area=25%–75%; grade 4, affected area>75%) as previously described.[42]

Glomerular Isolation

Mice were anesthetized and perfused through the heart with magnetic 4.5-μm-diameter Dynabeads (Invitrogen). Kidneys were minced into small pieces, digested by collagenase A (Roche), filtered, and collected using a magnet.[43]

Quantitative RT-PCR

Total RNA (1 μg) was reverse-transcribed into cDNA. Each reaction was done in duplicate. The quantity of cDNA in each sample was normalized to the amount of *Hprt* cDNA. For the PCR, we used SYBR Premix Ex Taq II (TAKARA Bio) according to the manufacturer's instructions. The amplification was carried out in a Thermal Cycler Dice Real Time System (TAKARA Bio). The following primer pairs were used: *Mafb*, 5′-TGAGCATGGGGCAAGAGCTG-3′ and 5′-CCATCCAGTACAGGTCCTCG-3′; *Nphs1*, 5′-GCCACCACCTTCACACTGAC-3′ and 5′-AGACCACCAACCGCAAAGA-3′; *Nphs2*, 5′-GGGCATCAAAGTGGAGAGAACTG-3′ and 5′-TGGACAGCGACTGAAGAGTGTG-3′; *Podxl*, 5′-GAGCACAGCGAGCCATCC-3′ and 5′-GTGGAGACGGGCAATGTAG-3′; *Gpx1*, 5′-GGTTCGAGCCCAATTTTACA-3′ and 5′-CCCACCAGGAACTTCTCAAA-3′; *Gpx3*, 5′-GATGTGAACGGGGAGAAAGA-3′ and 5′-CCCACCAGGAACTTCTCAAA-3′; *Gpx4*, 5′-CTCCATGCACGAATTCTCAG-3′ and 5′-ACGTCAGTTTTGCCTCATTG-3′; *Notch1*, 5′-ATGGCATCGCGGGCTTCACTT-3′ and 5′-TCCTTGCATACCCCGCTGTTTTTG-3′; *Notch2*, 5′-CATTGACGAGTGCACTGA-3′ and 5′-GAGTGCTGGCACAAGTGT-3′; *Notch3*, 5′-GTGGATGTCAACGTCCGA-3′ and 5′-TGCCAGGATCAGTGCAGT-3′; *Notch4*, 5′-CAGAACGTGGATCCCCTCAAGTTGC-3′ and 5′-AGGCAGAGAGAGGGCAAGGACTCAT-3′; *Jag1*, 5′-CGGTGGCTGGGAAGGAA-3′ and 5′-CTCGGGCCACACCAGAC-3′; *Dll1*, 5′-GGCTCTTCCCCTTGTTCTAAC-3′ and 5′-CTTCAGCCGGACGCAGACC-3′; *Hes1*, 5′-AAAGACGGCCTCTGAGCACA-3′ and 5′-TCATGGCGTTGATCTGGGTCA-3′; *Hey1*, 5′-GGGAGGGTCAGCAAAGCA-3′ and 5′-GCTGCGCATCTGATTTGTCA-3′; *Hprt*, 5′-TTGTTGTTGGATATGCCCTTGACTA-3′ and 5′-AGGCAGATGGCCACAGGACTA -3′.[44–46]

Luciferase Assay

To construct reporter plasmids, DNA fragments corresponding to positions −427 to +173 in the WT and mutant murine Nephrin gene promoter[18] were PCR-amplified and subcloned into the pGL3-Luc vector (Promega, Madison, WI). To express Mafb, we used a previously described expression plasmid (pEFX3-FLAG-Mafb).[47] Reporter and effecter plasmids were transfected into 293T cells by lipofection using FuGENE6 transfection regent (Roche) and then harvested 24 hours post-transfection. Luciferase assays were performed according to the manufacturer's protocol using the Dual-Luciferase Reporter Assay System (Promega). Transfection efficiency was routinely monitored and normalized using the coexpressed *Renilla reniformis* luciferase

activity, which was expressed from the pRL-TK (Promega) expression plasmid.

EMSA

Biotin labeling of oligonucleotide probes and protein–DNA binding reactions were performed using the LightShift chemiluminescent EMSA kit (Thermo Fisher Scientific, Rockford, IL) according to the manufacturer's directions. Mafb and mock-control proteins were prepared from 293T cells transiently transfected with expression vectors, pEFX3-FLAG-Mafb or pEFX3-FLAG mock, as previously described.[48] Nuclear extracts were incubated with the biotin-labeled probe and a reaction mixture containing 10 mM Tris, 50 mM KCl, 1 mM dithiothreitol, 5 mM $MgCl_2$, 50 ng/L poly (dI–dC), 0.05% NP-40, and 2.5% glycerol for 20 minutes at room temperature. The oligonucleotide probes containing the MARE sequences are as follows: consensus MARE sequence: 5′-AGCTCGGAATTGCTGACTCATCATTACTC-3′ and 3′-TCGAGCCTTAACGACTGAGTAGTAATGAG-5′; Nephrin-MARE: 5′-GTTCCTGGCATGTGCTGACAGGGGATTTC-3′ and 3′-CAAGGACCGTACACGACTGTCCCCTAAAG-5′. A 200-fold excess of unlabeled oligonucleotide was added to the reaction mixture for competition studies. Anti- Mafb antibody (BL658; Bethyl) was preincubated with the extract protein for 10 minutes before incubation of the biotin-labeled probe to detect each protein.

Measurement of Urinary Levels of 8-OHdG

The urinary excretion of 8-OHdG was measured by competitive ELISA using a commercially available kit: New 8-OHdG Check (Japan Institute for the Control of Aging, Shizuoka, Japan).

Measurement of Glutathione Peroxidase Activity

Collected glomeruli were subjected to glutathione peroxidase assays according to the manufacturer's instructions. Glutathione peroxidase assays kits and reagents were all purchased from Cayman Chemical Company (Ann Arbor, MI).

Cell Culture

Mouse podocytes (SVI) from a conditionally immortalized cell line were obtained from CLS.[49] Cells were grown in RPMI 1640 medium (Gibco, Grand Island, NY) supplemented with 10% FBS, penicillin (100 units/L), and streptomycin (100 mg/L) in a controlled humidified atmosphere. To propagate podocytes, the culture medium was supplemented with 10 units/ml mouse recombinant IFN-γ, and the cells were cultivated at 33°C to enhance the expression of the temperature-sensitive large T antigen (permissive conditions). To induce differentiation, podocytes were maintained at 37°C without IFN-γ (nonpermissive conditions) for 7 days.[50]

Cell Transfection

One day before transfection, the culture medium was removed, and cells were cultivated in antibiotic-free RPMI 1640 (Gibco) supplemented with 10% FBS. The cells were transfected with expression vectors, pEFX3-FLAG-Mafb or pEFX3-FLAG mock, using Lipofectamine LTX (Life Technologies, Carlsbad, CA) according to the manufacturer's instructions. The cells were incubated an additional 24 hours. Transfected cells were cultured in normal (5.5 mM) and high (30 mM) glucose concentration for 72 hours. Subsequently, Western blot analysis and quantitative RT-PCR were performed.

Western Blot Analysis of Podocytes

Podocytes were treated with lysis buffer (20 mM Tris, 140 mM NaCl, 2 mM EDTA, 10% glycerol, and 1% Nonidet P-40) in the presence of a protease inhibitor cocktail (Sigma-Aldrich) and then homogenized at 4°C by scraping. The homogenates were centrifuged at 9500×g for 20 minutes at 4°C, and supernatants were used as sample proteins. Equal amounts of protein, containing 20 μg, were separated on a SDS–polyacrylamide gel (10%) and transferred to Immobilon-P PVDF Membrane (EMD Millipore). The following antibodies were used for Western blotting: anti-Mafb (Bethyl), anti-Gpx3 (H-10; Santa Cruz Biotechnology), anti-Notch2 (D76A6, Cell Signal Technology, Danvers, MA), and anti–β-actin (horseradish peroxidase–conjugate; 13E5; Cell Signaling Technology). Blots were developed by using the Pierce Fast Western Blot Kit, and the signals were captured on an image reader (Las-3000; FujiFilm, Tokyo, Japan). Amount of proteins was determined from the blot with ImageJ.

Podocyte Number Counting

Kidney sections (4 μm) were immunostained with a polyclonal antibody against WT1 (C-19; Santa Cruz Biotechnology) as the primary antibody and detected by the avidin-biotin-peroxidase complex staining technique using a Histofine Kit (Nichirei, Tokyo, Japan). Podocyte density was determined from a count of the number of WT1-positive nuclei per glomerular section.

TUNEL Assay

Apoptotic cells were estimated by the TUNEL assay, which relies on incorporation of labeled 2′-deoxyuridine, 5′-triphosphate at sites of DNA breaks. For the TUNEL procedure, all reagents, including buffer, were part of a kit (*In Situ* TAKARA Apoptosis Kit; TAKARA Bio) applied to frozen kidney sections. Procedures were carried out according to the manufacturer's instructions. For identification of apoptotic podocytes, the kidney sections were costained with WT1 antibody (C-19; Santa Cruz Biotechnology) and 4′,6-diamidino-2-phenylindole. Apoptosis was examined in 4-μm-thick sections of the kidneys. For quantitative histologic analysis, the degree of apoptosis was estimated using a scale based on the mean number of TUNEL-positive cells per 100 glomerular sections.

Statistical Analyses

All results were expressed as means±SEMs. Multiple data comparisons were conducted using the one-way ANOVA with the Bonferroni correction. Significant differences between the two groups of mice were analyzed using the unpaired t test. Differences were considered statistically significant at P values <0.05.

ACKNOWLEDGMENTS

This work was supported by The Japan Society for the Promotion of Science KAKENHI Grant-in-Aid for Scientific Research 24591223.

DISCLOSURES

None.

REFERENCES

1. Jefferson JA, Shankland SJ, Pichler RH: Proteinuria in diabetic kidney disease: A mechanistic viewpoint. *Kidney Int* 74: 22–36, 2008
2. Pavenstädt H, Kriz W, Kretzler M: Cell biology of the glomerular podocyte. *Physiol Rev* 83: 253–307, 2003
3. Pagtalunan ME, Miller PL, Jumping-Eagle S, Nelson RG, Myers BD, Rennke HG, Coplon NS, Sun L, Meyer TW: Podocyte loss and progressive glomerular injury in type II diabetes. *J Clin Invest* 99: 342–348, 1997
4. Isermann B, Vinnikov IA, Madhusudhan T, Herzog S, Kashif M, Blautzik J, Corat MA, Zeier M, Blessing E, Oh J, Gerlitz B, Berg DT, Grinnell BW, Chavakis T, Esmon CT, Weiler H, Bierhaus A, Nawroth PP: Activated protein C protects against diabetic nephropathy by inhibiting endothelial and podocyte apoptosis. *Nat Med* 13: 1349–1358, 2007
5. Susztak K, Raff AC, Schiffer M, Böttinger EP: Glucose-induced reactive oxygen species cause apoptosis of podocytes and podocyte depletion at the onset of diabetic nephropathy. *Diabetes* 55: 225–233, 2006
6. Meyer TW, Bennett PH, Nelson RG: Podocyte number predicts long-term urinary albumin excretion in Pima Indians with Type II diabetes and microalbuminuria. *Diabetologia* 42: 1341–1344, 1999
7. Fredersdorf S, Weil J, Ulucan C, Birner C, Büttner R, Schubert T, Böger CA, Debl K, Muders F, Riegger GA, Luchner A: Vasopeptidase inhibition attenuates proteinuria and podocyte injury in Zucker diabetic fatty rats. *Naunyn Schmiedebergs Arch Pharmacol* 375: 95–103, 2007
8. Kataoka K, Fujiwara KT, Noda M, Nishizawa M: MafB, a new Maf family transcription activator that can associate with Maf and Fos but not with Jun. *Mol Cell Biol* 14: 7581–7591, 1994
9. Kataoka K, Noda M, Nishizawa M: Maf nuclear oncoprotein recognizes sequences related to an AP-1 site and forms heterodimers with both Fos and Jun. *Mol Cell Biol* 14: 700–712, 1994
10. Moriguchi T, Hamada M, Morito N, Terunuma T, Hasegawa K, Zhang C, Yokomizo T, Esaki R, Kuroda E, Yoh K, Kudo T, Nagata M, Greaves DR, Engel JD, Yamamoto M, Takahashi S: MafB is essential for renal development and F4/80 expression in macrophages. *Mol Cell Biol* 26: 5715–5727, 2006
11. Zankl A, Duncan EL, Leo PJ, Clark GR, Glazov EA, Addor MC, Herlin T, Kim CA, Leheup BP, McGill J, McTaggart S, Mittas S, Mitchell AL, Mortier GR, Robertson SP, Schroeder M, Terhal P, Brown MA: Multicentric carpotarsal osteolysis is caused by mutations clustering in the amino-terminal transcriptional activation domain of MAFB. *Am J Hum Genet* 90: 494–501, 2012
12. Fan Q, Shike T, Shigihara T, Tanimoto M, Gohda T, Makita Y, Wang LN, Horikoshi S, Tomino Y: Gene expression profile in diabetic KK/Ta mice. *Kidney Int* 64: 1978–1985, 2003
13. Wong MA, Cui S, Quaggin SE: Identification and characterization of a glomerular-specific promoter from the human nephrin gene. *Am J Physiol Renal Physiol* 279: F1027–F1032, 2000
14. Menne J, Meier M, Park JK, Boehne M, Kirsch T, Lindschau C, Ociepka R, Leitges M, Rinta-Valkama J, Holthofer H, Haller H: Nephrin loss in experimental diabetic nephropathy is prevented by deletion of protein kinase C alpha signaling in-vivo. *Kidney Int* 70: 1456–1462, 2006
15. Nadarajah R, Milagres R, Dilauro M, Gutsol A, Xiao F, Zimpelmann J, Kennedy C, Wysocki J, Batlle D, Burns KD: Podocyte-specific overexpression of human angiotensin-converting enzyme 2 attenuates diabetic nephropathy in mice. *Kidney Int* 82: 292–303, 2012
16. Guo G, Morrison DJ, Licht JD, Quaggin SE: WT1 activates a glomerular-specific enhancer identified from the human nephrin gene. *J Am Soc Nephrol* 15: 2851–2856, 2004
17. Moeller MJ, Sanden SK, Soofi A, Wiggins RC, Holzman LB: Two gene fragments that direct podocyte-specific expression in transgenic mice. *J Am Soc Nephrol* 13: 1561–1567, 2002
18. Deb DK, Wang Y, Zhang Z, Nie H, Huang X, Yuan Z, Chen Y, Zhao Q, Li YC: Molecular mechanism underlying 1,25-dihydroxyvitamin D regulation of nephrin gene expression. *J Biol Chem* 286: 32011–32017, 2011
19. Shirota S, Yoshida T, Sakai M, Kim JI, Sugiura H, Oishi T, Nitta K, Tsuchiya K: Correlation between the expression level of c-maf and glutathione peroxidase-3 in c-maf -/- mice kidney and c-maf overexpressed renal tubular cells. *Biochem Biophys Res Commun* 348: 501–506, 2006
20. Granqvist A, Nilsson UA, Ebefors K, Haraldsson B, Nyström J: Impaired glomerular and tubular antioxidative defense mechanisms in nephrotic syndrome. *Am J Physiol Renal Physiol* 299: F898–F904, 2010
21. Park SJ, Lee BH, Kim DJ: Identification of proteins that interact with podocin using the yeast 2-hybrid system. *Yonsei Med J* 50: 273–279, 2009
22. Chen HC, Guh JY, Lai YH: Alterations of glomerular and extracellular glutathione peroxidase levels in patients and rats with focal segmental glomerulosclerosis. *J Lab Clin Med* 137: 279–283, 2001
23. de Haan JB, Stefanovic N, Nikolic-Paterson D, Scurr LL, Croft KD, Mori TA, Hertzog P, Kola I, Atkins RC, Tesch GH: Kidney expression of glutathione peroxidase-1 is not protective against streptozotocin-induced diabetic nephropathy. *Am J Physiol Renal Physiol* 289: F544–F551, 2005
24. van Stralen E, van de Wetering M, Agnelli L, Neri A, Clevers HC, Bast BJ: Identification of primary MAFB target genes in multiple myeloma. *Exp Hematol* 37: 78–86, 2009
25. Niranjan T, Bielesz B, Gruenwald A, Ponda MP, Kopp JB, Thomas DB, Susztak K: The Notch pathway in podocytes plays a role in the development of glomerular disease. *Nat Med* 14: 290–298, 2008
26. Sharma S, Sirin Y, Susztak K: The story of Notch and chronic kidney disease. *Curr Opin Nephrol Hypertens* 20: 56–61, 2011
27. Connor A, Highton J, Hung NA, Dunbar J, MacGinley R, Walker R: Multicentric carpal-tarsal osteolysis with nephropathy treated successfully with cyclosporine A: A case report and literature review. *Am J Kidney Dis* 50: 649–654, 2007
28. Doublier S, Salvidio G, Lupia E, Ruotsalainen V, Verzola D, Deferrari G, Camussi G: Nephrin expression is reduced in human diabetic nephropathy: Evidence for a distinct role for glycated albumin and angiotensin II. *Diabetes* 52: 1023–1030, 2003
29. Bonnet F, Tikellis C, Kawachi H, Burns WC, Wookey PJ, Cao Z, Cooper ME: Nephrin expression in the post-natal developing kidney in normotensive and hypertensive rats. *Clin Exp Hypertens* 24: 371–381, 2002
30. Quack I, Woznowski M, Potthoff SA, Palmer R, Königshausen E, Sivritas S, Schiffer M, Stegbauer J, Vonend O, Rump LC, Sellin L: PKC alpha mediates beta-arrestin2-dependent nephrin endocytosis in hyperglycemia. *J Biol Chem* 286: 12959–12970, 2011
31. Forbes JM, Coughlan MT, Cooper ME: Oxidative stress as a major culprit in kidney disease in diabetes. *Diabetes* 57: 1446–1454, 2008
32. Obrosova IG, Fathallah L, Liu E, Nourooz-Zadeh J: Early oxidative stress in the diabetic kidney: Effect of DL-alpha-lipoic acid. *Free Radic Biol Med* 34: 186–195, 2003
33. Gui D, Guo Y, Wang F, Liu W, Chen J, Chen Y, Huang J, Wang N: Astragaloside IV, a novel antioxidant, prevents glucose-induced podocyte apoptosis in vitro and in vivo. *PLoS ONE* 7: e39824, 2012
34. Calderón-Salinas JV, Muñoz-Reyes EG, Guerrero-Romero JF, Rodríguez-Morán M, Bracho-Riquelme RL, Carrera-Gracia MA, Quintanar-Escorza MA: Eryptosis and oxidative damage in type 2 diabetic mellitus patients with chronic kidney disease. *Mol Cell Biochem* 357: 171–179, 2011
35. Zhang W, Miao J, Wang S, Zhang Y: The protective effects of beta-casomorphin-7 against glucose -induced renal oxidative stress in vivo and vitro. *PLoS ONE* 8: e63472, 2013

36. Ahn SH, Susztak K: Getting a notch closer to understanding diabetic kidney disease. *Diabetes* 59: 1865–1867, 2010
37. Waters AM, Wu MY, Huang YW, Liu GY, Holmyard D, Onay T, Jones N, Egan SE, Robinson LA, Piscione TD: Notch promotes dynamin-dependent endocytosis of nephrin. *J Am Soc Nephrol* 23: 27–35, 2012
38. Murea M, Park JK, Sharma S, Kato H, Gruenwald A, Niranjan T, Si H, Thomas DB, Pullman JM, Melamed ML, Susztak K: Expression of Notch pathway proteins correlates with albuminuria, glomerulosclerosis, and renal function. *Kidney Int* 78: 514–522, 2010
39. Chu D, Zhang Z, Zhou Y, Wang W, Li Y, Zhang H, Dong G, Zhao Q, Ji G: Notch1 and Notch2 have opposite prognostic effects on patients with colorectal cancer. *Ann Oncol* 22: 2440–2447, 2011
40. Brunskill EW, Georgas K, Rumballe B, Little MH, Potter SS: Defining the molecular character of the developing and adult kidney podocyte. *PLoS ONE* 6: e24640, 2011
41. Machiya J, Shibata Y, Yamauchi K, Hirama N, Wada T, Inoue S, Abe S, Takabatake N, Sata M, Kubota I: Enhanced expression of MafB inhibits macrophage apoptosis induced by cigarette smoke exposure. *Am J Respir Cell Mol Biol* 36: 418–426, 2007
42. Ren XJ, Guan GJ, Liu G, Zhang T, Liu GH: Effect of activin A on tubulointerstitial fibrosis in diabetic nephropathy. *Nephrology (Carlton)* 14: 311–320, 2009
43. Takemoto M, Asker N, Gerhardt H, Lundkvist A, Johansson BR, Saito Y, Betsholtz C: A new method for large scale isolation of kidney glomeruli from mice. *Am J Pathol* 161: 799–805, 2002
44. Barnes KM, Evenson JK, Raines AM, Sunde RA: Transcript analysis of the selenoproteome indicates that dietary selenium requirements of rats based on selenium-regulated selenoprotein mRNA levels are uniformly less than those based on glutathione peroxidase activity. *J Nutr* 139: 199–206, 2009
45. Sunde RA, Raines AM, Barnes KM, Evenson JK: Selenium status highly regulates selenoprotein mRNA levels for only a subset of the selenoproteins in the selenoproteome. *Biosci Rep* 29: 329–338, 2009
46. Nyfeler Y, Kirch RD, Mantei N, Leone DP, Radtke F, Suter U, Taylor V: Jagged1 signals in the postnatal subventricular zone are required for neural stem cell self-renewal. *EMBO J* 24: 3504–3515, 2005
47. Kajihara M, Sone H, Amemiya M, Katoh Y, Isogai M, Shimano H, Yamada N, Takahashi S: Mouse MafA, homologue of zebrafish somite Maf 1, contributes to the specific transcriptional activity through the insulin promoter. *Biochem Biophys Res Commun* 312: 831–842, 2003
48. Nakamura M, Hamada M, Hasegawa K, Kusakabe M, Suzuki H, Greaves DR, Moriguchi T, Kudo T, Takahashi S: c-Maf is essential for the F4/80 expression in macrophages in vivo. *Gene* 445: 66–72, 2009
49. Schiwek D, Endlich N, Holzman L, Holthöfer H, Kriz W, Endlich K: Stable expression of nephrin and localization to cell-cell contacts in novel murine podocyte cell lines. *Kidney Int* 66: 91–101, 2004
50. Piwkowska A, Rogacka D, Audzeyenka I, Jankowski M, Angielski S: High glucose concentration affects the oxidant-antioxidant balance in cultured mouse podocytes. *J Cell Biochem* 112: 1661–1672, 2011

Therapeutic Apheresis and Dialysis

Successful Use of Tocilizumab in a Case of Multicentric Castleman's Disease and End-Stage Renal Disease

Dear Editor,

Castleman's disease (CD) is a uni- or multicentric lymphoproliferative disorder that is characterized by interleukin 6 (IL-6) production from proliferated lymph node tissue and that can show systemic involvement (1). Patients with CD typically receive chemotherapy and corticosteroids according to malignant lymphoma regimens; in the absence of therapy, CD carries a grave prognosis, with complications including infection, malignancy, and renal failure (1). However, no specific therapy has been recommended for CD in the face of end-stage renal disease (ESRD), despite the prevalence of various adverse conditions in CD patients receiving hemodialysis. The recombinant anti-IL-6 receptor antibody tocilizumab (2) has been used to treat rheumatoid arthritis, juvenile rheumatoid arthritis, and CD in Japan. Efficiency and safety of administration of tocilizumab in a patient with AA amyloidosis (3) or rheumatoid arthritis (4) receiving hemodialysis was recently described. In light of its mode of action and efficacy in patients with CD, we suggest that tocilizumab may be useful for patients with CD and ESRD and here report an illustrative case.

A 65-year-old man, who was diagnosed as having the plasma-cell type of multicentric CD in 2003, was admitted to our hospital for severe anemia in October 2012. Despite receiving prednisolone, cyclophosphamide, and ritximab since diagnosis of CD, his disease had progressed to renal involvement and ESRD; he began hemodialysis in 2006. His admission examination in 2012 revealed no abnormalities except cervical lymphadenopathy. In addition, our patient had severe normocytic anemia (Hgb, 6.6 g/dL) despite receiving 120 μg darbepoetin-α weekly; serum biochemical studies revealed hypergammoglobulinemia (IgG, 4454 mg/dL; IgA, 938 mg/dL; IgM, 94 mg/dL) and excess IL-6 (38.1 pg/mL).

In view of our patient's history of ischemic heart disease, diabetes, and glaucoma, we were reluctant to pursue additional prednisolone or chemotherapy. According to institutional policy, we screened our patient and found him to be clear of infection; he then began treatment with tocilizumab (8 mg/kg biweekly) in October 2012. IgG and Hgb levels gradually normalized, and levels of CRP decreased; we then successfully decreased the dose of darbepoetin-α (Fig. 1). As noted previously, decreasing the inflammation increased hematopoiesis, and ferritin and serum iron levels decreased accordingly (5).

Serum IL-6 became extremely elevated (>1700 pg/dL) upon the administration of tocilizumab, likely due to saturation of the IL-6 receptor (6); this phenomenon occurs regardless of whether CD is accompanied by hemodialysis or ESRD. Our patient has experienced no serious complication (e.g., infection, anaphylaxis) during 6 months of follow-up and continued tocilizumab therapy. In some literature, therapeutic responses with rituximab are partial regression in CD (7,8). To our knowledge, there is no direct evidence to show which is more effective between rituximab and tocilizumab. In our case, CD seems to be successfully regulated by tocilizumab targeting disease specific cytokine; IL-6 rather than tocilizmab broadly targeting B cells. We conclude that tocilizumab is a potential therapeutic strategy for Castleman's disease with end-stage renal disease.

Kei Nagai,[1,2] Atsushi Ueda,[2] and Kunihiro Yamagata[1]

[1]Departments of Nephrology, Faculty of Medicine, University of Tsukuba, Tsukuba, and [2]Kidney and Dialysis Center, Namegata Distinct General Hospital, Namegata, Ibaraki, Japan

Email: minkei@hotmail.co.jp

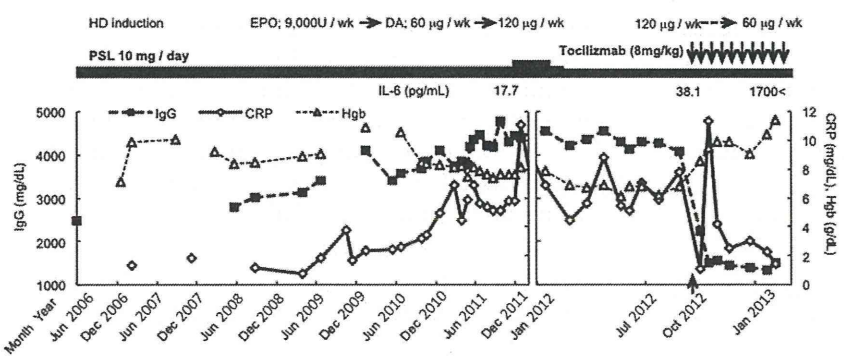

FIG. 1. The clinical course of the presented case. Our patient had received prednisolone (PSL, 10 mg daily) and tocilizumab (8 mg/kg twice weekly) since October 2012. CRP, C-reactive protein; DA, darbepoetin-α; EPO, erythropoetin; HD, hemodialysis; Hgb, hemoglobin; IgG, immunoglobulin G.

REFERENCES

1. Peterson BA, Frizzera G. Multicentric Castleman's disease. *Semin Oncol* 1993;20:636–47.
2. Nishimoto N, Kanakura Y, Aozasa K et al. Humanized anti-interleukin-6 receptor antibody treatment of multicentric Castleman disease. *Blood* 2005;106:2627–32.
3. Hattori Y, Ubara Y, Sumida K et al. Tocilizumab improves cardiac disease in a hemodialysis patient with AA amyloidosis secondary to rheumatoid arthritis. *Amyloid* 2012;19:37–40.
4. Iwamoto M, Honma S, Asano Y, Minota S. Effective and safe administration of tocilizumab to a patient with rheumatoid arthritis on haemodialysis. *Rheumatol Int* 2011;31:559–60.
5. Kawabata H, Tomosugi N, Kanda J, Tanaka Y, Yoshizaki K, Uchiyama T. Anti-interleukin 6 receptor antibody tocilizumab reduces the level of serum hepcidin in patients with multicentric Castleman's disease. *Haematologica* 2007;92:857–8.
6. Nishimoto N, Terao K, Mima T, Nakahara H, Takagi N, Kakehi T. Mechanisms and pathologic significances in increase in serum interleukin-6 (IL-6) and soluble IL-6 receptor after administration of an anti-IL-6 receptor antibody, tocilizumab, in patients with rheumatoid arthritis and Castleman disease. *Blood* 2008;112:3959–64.
7. Van Rhee F, Stone K, Szmania S, Barlogie B, Singh Z. Castleman disease in the 21st century: an update on diagnosis, assessment, and therapy. *Clin Adv Hematol Oncol* 2010;8:486–98.
8. Bower M, Powles T, Williams S et al. Brief communication: rituximab in HIV-associated multicentric Castleman disease. *Ann Intern Med* 2007;147:836–9.

Vaginal Leakage of Peritoneal Dialysate in a Peritoneal Dialysis Patient

Dear Editor,

Dialysate leakage represents a noninfectious complication of peritoneal dialysis (PD), with an incidence of approximately 5% in PD patients. Vaginal leakage of peritoneal fluid is very rare. We report a case of a woman who developed vaginal leakage during CAPD.

A 25-year-old female patient treated with PD for the last 2 years with diagnosis of end stage renal disease (ESRD) secondary to vesico-ureteric reflux (VUR) admitted to our outpatient clinic with the complaint of vaginal fluid leakage for 15 days. Biochemical analysis of the fluid coming from the vagina and the dialysate was similar (vaginal fluid glucose 1977 mg/dL, dialysate glucose 2039 mg/dL). Computed tomography (CT) peritoneography was performed using 100 mL iopamidol (370 mg/mL) mixed with 2000 mL dialysate, which was then infused into the peritoneal cavity via the PD catheter. CT images were taken 30 min after contrast infusion. CT peritoneography showed that the contrast material mainly accumulated in the peritoneal pouch particularly around the peritoneal dialysis catheter. Additionally, the passage of contrast material into the endometrial cavity was noted, the vagina and both fallopian tubes were filled with contrast material (Fig. 1). It was considered that contrast material had a retrograde passage into the endometrial cavity through the fallopian tubes. PD treatment was stopped and she was switched to hemodialysis.

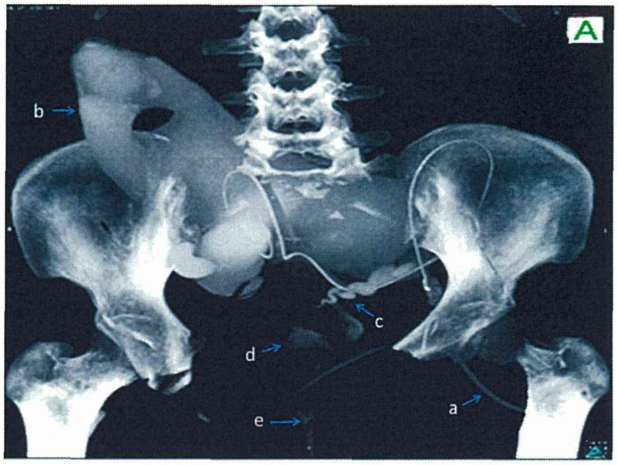

FIG. 1. Computed tomography (CT) peritoneography demonstrates leakage through fallopian tubes (c) and the contrast agent shows accumulation of the dialysis solution in a subcompartment (b); tenckhoff catheter (a), endometrial cavity (d), vagina (e).

Vaginal leakage of dialysate is one of the late and uncommon complications of PD and usually occurs in adult patients. Multiple surgical operations, use of steroids, hypothyroidism, polycystic kidney disease, recurrent peritonitis, obesity, and high dialysate volume may cause abdominal wall weakness, hernias, and high intra-abdominal pressure. These are the main predisposing factors for dialysate leaks (1–3). Our patient presented vaginal leakage with no genital tract abnormalities.

Peritoneal scintigraphy, CT peritoneography, and magnetic resonance peritoneography are the diagnostic procedures that can be used in the investigation of suspected leaks or hernias in patients on PD (4). In this patient, we preferred CT peritoneography with intraperitoneal administration of contrast agent. Treatments for dialysate leaks include surgical repair, temporary or permanent transfer to hemodialysis, continuing PD with lower dialysate volumes, or performing PD with a cycler (2). There is no consensus on the selection of treatment options. Our patient was transferred to hemodialysis permanently.

In conclusion, vaginal leakage of dialysate is one of the late and uncommon complications of PD. This complication should be suspected in women with genital leakage on PD treatment.

We have no financial disclosures to declare and no conflicts of interest to report.

Human Pathology (2014) 45, 1918–1927

ELSEVIER

Human PATHOLOGY

www.elsevier.com/locate/humpath

Original contribution

Clinicopathological spectrum of kidney diseases in cancer patients treated with vascular endothelial growth factor inhibitors: a report of 5 cases and review of literature ☆

Joichi Usui MD, PhD [a,b], Ilya G. Glezerman MD [c], Steven P. Salvatore MD [a], Chandra B. Chandran MD [d], Carlos D. Flombaum MD [c], Surya V. Seshan MD [a,*]

[a] *Department of Pathology, Weill Cornell Medical College, Cornell University, New York, New York, 10065*
[b] *Department of Nephrology, Faculty of Medicine, University of Tsukuba, Tsukuba, Ibaraki, 305–8575, Japan*
[c] *Renal Service, Department of Medicine, Memorial Sloan-Kettering Cancer Center, New York, New York, 10065*
[d] *Nephrology Division, Department of Medicine, St. Joseph's Regional Medical Center, Paterson, New Jersey, 07503*

Received 11 April 2014; revised 21 May 2014; accepted 28 May 2014

Keywords:
Vascular endothelial growth factor inhibitor;
Thrombotic microangiopathy;
Acute tubular injury;
Proteinuria;
Renal failure

Summary Recently, cancer therapies have been supplemented by vascular endothelial growth factor (VEGF) inhibitors as anti-angiogenic agents. However, kidney-related adverse reactions associated with these agents clinically manifest as hypertension and proteinuria, the most severe form being thrombotic microangiopathy (TMA). We present the spectrum of pathological features in VEGF inhibitor-associated kidney disease. Clinicopathological findings of kidney disease were retrospectively studied in 5 cancer patients treated with anti-VEGF agents. Although 4 cases received bevacizumab (anti–VEGF-A), one was given sorafenib (small molecule tyrosine kinase inhibitor affecting VEGF-R2). All patients presented with acute kidney injury, hypertension, and/or proteinuria. All kidney biopsies showed recent and chronic endothelial injury of varying severity and vascular sclerosis, including 2 with typical active features of TMA. Furthermore, acute tubular injury with focal necrosis was seen in all cases. While administration of VEGF inhibitor was discontinued in 4 cases, it was resumed for 5 more doses, following steroid therapy in 1 case. Cessation of VEGF inhibitor therapy was successful in reversing anemia and led to improvement of hypertension and proteinuria in 4 of the 5 cases. One case with TMA progressed to end-stage renal disease. A range of renal pathologic lesions secondary to endothelial injury are noted often accompanied by acute tubular damage following anti-VEGF therapy, the most severe being TMA. While most of the clinical manifestations are reversible with discontinuation of therapy, the role of other nephrotoxic chemotherapeutic agents in enhancing renal injury including severe TMA and other host factors with possible poor outcome should be considered.

1. Introduction

Vascular endothelial growth factor (VEGF) signal transduction is crucial as a regulatory system of vascular

☆ Statement of financial interests: None.

* Corresponding author. 525 East 68th St, Box 69, New York NY 10065.
E-mail address: svs2002@med.cornell.edu (S. V. Seshan).

http://dx.doi.org/10.1016/j.humpath.2014.05.015
0046-8177/